Desalination and Water Treatment
www.deswater.com

doi: 10.5004/dwt.2022.28321

255 (2022) 56–67
April

Swelling and adsorption properties of crosslinked chitosan-based films: kinetic, thermodynamic and optimization studies

Nacer Boudouaia[a], Ahmed Amine Bendaoudi[a], Hacene Mahmoudi[b], Taoufiq Saffaj[c], Zohra Bengharez[a,*]

[a]*Laboratory of Advanced Materials and Physico-Chemistry for Environment and Health, Djillali Liabes University of Sidi Bel Abbes, 22000, Algeria, Tel. +213 5 41 76 15 78; emails: dzbengharez@yahoo.fr (Z. Bengharez), boudouaianacer@yahoo.fr (N. Boudouaia), bendaoudi22@hotmail.fr (A.A. Bendaoudi)*
[b]*Faculty of Technology, University Hassiba Benbouali of Chlef, Chlef 02000, Algeria, email: h.mahmoudi@univ-chlef.dz*
[c]*Laboratory of Applied Organic Chemistry, University Sidi Mohamed Ben Abdellah, Fes, Morocco, email: taoufiq.saffaj@usmba.ac.ma*

Received 16 November 2021; Accepted 26 December 2021

ABSTRACT

The study was aimed at synthesizing films of crosslinked chitosan-terephthaldehyde (CS-TPA) and investigating their swelling, adsorption, kinetic, isotherm and thermodynamic properties. Films derived from CS-TPA were prepared with different cross-linking rates of 0%, 0.1% and 0.2%. The chemical composition of the films was examined using Fourier-transform infrared spectrometry to confirm formation of Schiff base. The morphology of films was analyzed by scanning electron microscopy. The micrographs showed that the chitosan (CS) films had a homogeneous smooth surface while CS-TPA films had cavities which were related to the cross-linking rate. Thermal properties were characterized by differential scanning calorimetry analysis where results revealed that synthesized films had degradation and glass transition temperatures in agreement with the literature. The swelling behavior of the films was examined by varying the cross-linking rate, reaction time, salinity, pH, and temperature. The swelling process of films was found to be endothermic and spontaneous and obeyed with a pseudo-second-order kinetic model. The adsorption performance of the crosslinked chitosan films was investigated for the removal of hexavalent chromium. The maximum adsorption capacity of 60.53 mg g^{-1} was obtained using terephthaldehyde 0.1%. The adsorption data fitted well to the Langmuir isotherm and a pseudo-second-order kinetic model. The thermodynamic results indicated that adsorption of chromium onto CS-TPA 0.1% film was favorable, spontaneous, and exothermic with high randomness at the solid/liquid interface.

Keywords: Chitosan; Terephthaldehyde; Cr(VI); Films; Swelling; Adsorption

1. Introduction

One of most serious environmental problems is heavy metal pollution of water. Among these pollutants, chromium is a widely used heavy metal in the tanning, textiles, electroplating, wood processing and even food industries [1]. In the aqueous phase, chromium exists mainly in two forms, hexavalent Cr(VI) and trivalent Cr(III). Species of Cr(VI) include aqueous forms H_2CrO_4, $HCrO_4^-$, $Cr_2O_7^{2-}$, CrO_4^{2-}, and solid forms CrO_3 [2]. Unlike Cr(III), the high solubility of Cr(VI) makes it more bio-available and more toxic to plants, aquatic organisms and humans [3].

Over the past decades, several chemical and/or biological technological methods have been employed for treatment of heavy metals. These approaches involve coagulation, ion exchange, precipitation, ultrafiltration, reverse osmosis

* Corresponding author.

Presented at the International Virtual Conference on Water and Energy (ICWE 21), Hassiba Benbouali University of Chlef, Algeria, 25–27 May 2021

and electrodialysis [4]. However, such techniques have various drawbacks, including very high reagent and energy consumption, expensive installations and equipment, mandatory monitoring systems and low selectivity. All of which translates into high cost. To circumvent these problems, adsorption has been applied for removal of Cr(VI) [5].

The development of new natural bio-adsorbents with or without modification has aroused great interest particularly in the case of chitosan (CS) which is an exceptional bio-sorbent for chromium [6], and is also a readily available polyaminosaccharide component of crustacean shells [7–9]. Chemically, it is a linear polycationic copolymer of 2-acetamido-2-deoxy-β-D-glucopyranose and 2-amino-2-deoxy-β-D-glucopyranose joined by β(1,4) glycosidic linkages obtained by deacetylation of chitin under alkaline conditions [10]. CS is odorless, biodegradable, non-allergenic and biocompatible [11–13]. It is antibacterial, renewable, non-toxic compound and widely used in biomedical applications [14,15] also in textiles, in wood products [16] and in wastewater treatment [17,18]. Furthermore, CS is a hydrophilic polymer present as an amorphous solid form soluble in acid solutions diluted by protonation of its amine groups (pKa = 6.5) at pH below 6 [19]. All these properties make chitosan a fascinating precursor for preparation of films [20].

The technique of separation by evaporation is one of most investigated fields for formation of films [21]. Liquid separation is controlled by chemical nature, morphology of film and experimental conditions of the process [22]. CS shows a swelling capacity in contact with aqueous media. To improve the mechanical and chemical properties of CS films, several studies have examined its modification by different methods, such as complexation and cross-linking [23]. CS cross-linking with dialdehydes has been subject of numerous studies [24,25] where terephthaldehyde (TPA) was employed as a crosslinking agent leading to different forms of chitosan (beads, films or membranes, gels, or hydrogels).

The aim of the present study was to prepare films of crosslinked chitosan-terephthaldehyde (CS-TPA) and then to investigate their swelling properties. Effects of cross-linking rate, reaction time, salinity, pH and temperature were assessed. Moreover, kinetic, and thermodynamic studies were carried out to optimize operating conditions for swelling. The second part was focused on assessing the kinetic, isotherm and thermodynamic effectiveness of CS-TPA 0.1% film in the removal of Cr(VI) from solution.

2. Materials and methods

2.1. Materials

Chitosan, CS was purchased from Sigma-Aldrich and terephthaldehyde was supplied by Riedel-de Haen. Acetic acid, sodium hydroxide and potassium dichromate used as a source of Cr(VI) ions were supplied by Sigma-Aldrich.

2.2. Preparation of films

Solution of 1% CS in acetic acid 0.17 M was poured into kneaded dishes (90/15 mm) and placed in an oven at 40°C for 36 h. The films thus obtained were removed from the mold and then neutralized with 0.1 N NaOH for 2 h, washed until neutralization. The resulting films were carefully removed and then dried in open air. The films were immersed in terephthaldehyde solution (0.1%, 0.2%, 0.4%, 0.6%) followed by washing with distilled water. The films were then dried at 50°C for 24 h and stored in a desiccator.

The cross-linking reaction between chitosan and terephthaldehyde is illustrated in Fig. 1.

Photographs of the CS-TPA films are shown in Fig. 2. The prepared films with cross-linking rates 0.4 and 0.6% were very fragile and brittle. The current study therefore focused on the first three films (Fig. 2a–c).

2.3. Characterization

The Fourier-transform infrared (FTIR) spectra of the films were recorded over a frequency range of 400–4,000 cm^{-1} using a FTIR spectra Bruker Alpha-P equipped with an ATR diamond (without solvent, without KBr). Thermal analysis was carried out by a differential scanning calorimeter (NETZSCH DSC 214 Polyma), where 10 mg of sample was put in crucible with a heating time and rate of 45 min and 10°C/min, respectively. The morphology of the products was determined by scanning electron microscope (SEM QUANTA 600). Kinetics adsorption of hexavalent chromium onto CS crosslinked were monitored using a Shimadzu UV-2401PC spectrophotometer at a wavelength λ = 540 nm.

2.3.1. pH at point of zero charge pH_{pzc}

The pH of the medium is one of the parameters that impacts the adsorption process since any change in pH affects the adsorbent surface. pH_{pzc} is the value of pH at which the sorbent surface charge is equal to zero. At pH < pH_{pzc}, the adsorbent surface is positively charged whereas at pH > pH_{pzc} the surface adopts a negative charge. The pH_{pzc} of the crosslinked chitosan film was determined using the pH drift salt addition method [8].

2.4. Swelling behavior study

Swelling ability is an important factor in assessing physical-chemical properties of films, Structural factors influencing swelling rate are time of reaction, cross-linking rate and hydrophily, as well as properties of medium such as pH, temperature, and salinity.

The swelling behavior of the synthesized films was followed by immersion of 1 cm^2 of dry films in distilled water at room temperature. Equilibrium swelling ratio of films was calculated using the following formula [26].

$$\% \text{ swelling} = \frac{w_s - w_d}{w_d} \times 100 \quad (1)$$

where w_s and w_d are the weight of the swollen and dry film respectively, at different swelling times.

2.5. Adsorption experiments of Cr(VI)

The adsorption efficiencies of Cr(VI) of the crosslinked chitosan-based films were investigated by batch adsorption

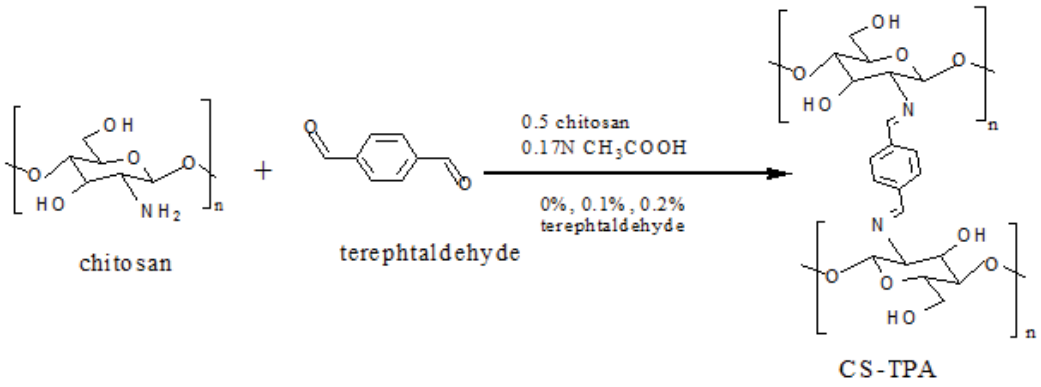

Fig. 1. Reaction of crosslinking CS-TPA film.

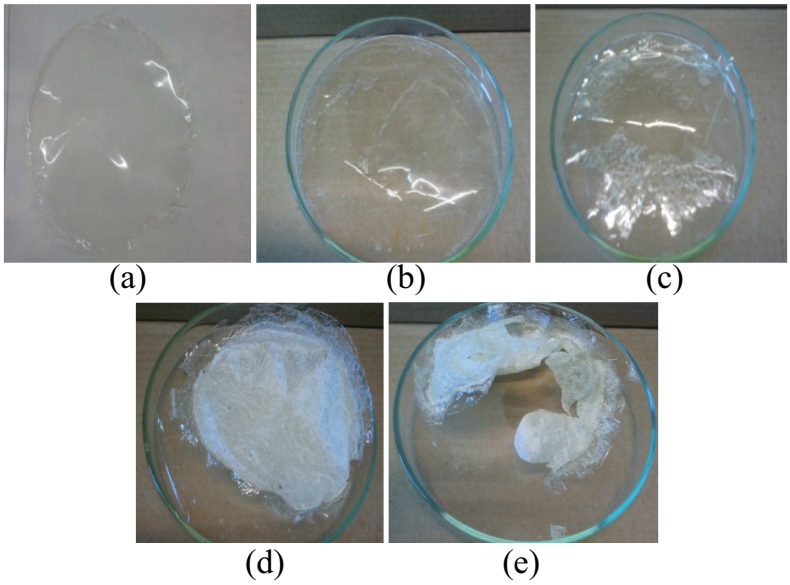

Fig. 2. Photographs of the synthesized films: (a) CS, (b) CS-TPA 0.1%, (c) CS-TPA 0.2%, (d) CS-TPA 0.4%, and (e) CS-TPA 0.6%.

experiments. In each experiment, 1 cm^2 of film was immersed in 100 mg L^{-1} of hexavalent chromium solution at neutral pH and room temperature. The amount of adsorbed Cr(VI) was calculated by applying Eq. (2):

$$q_t = \frac{c_i - c_t}{W} V \quad (2)$$

where q_t is amount of Cr(VI) absorbed (mg g^{-1}); c_i: initial Cr(VI) concentration (mg L^{-1}); c_t: Cr(VI) concentration after sorption (mg L^{-1}); W: mass of film (mg) and V: volume of solution. Kinetic modeling of hexavalent chromium adsorption was fitted with well-known models [27], namely pseudo-first-order and pseudo-second-order (Table 1).

2.6. Effect of parameters

The effect of initial hexavalent chromium concentration of 20, 30, 40 and 50 mg L^{-1} on its removal by CS-TPA film was assessed. These experiments were performed for fixed adsorbent surface 1 cm^2, aqueous pH at 20°C ± 2°C. The effect of pH on Cr(VI) efficiency was analyzed at various pH values ranging from 2 to 10 at 20°C ± 2°C, 50 mg L^{-1} of Cr(VI) and for contact time of 60 min. The effect of solution temperature on hexavalent chromium adsorption was investigated at different temperatures of 20°C, 30°C, 40°C and 50°C for an initial heavy metal concentration of 50 mg L^{-1} and a fixed contact time of 60 min.

2.7. Adsorption isotherms

An adsorption isotherm describes the relationship between amount of hexavalent chromium adsorbed by adsorbent film (CS-TPA) and concentration of remaining hexavalent chromium in solution at constant temperature. The adsorption mechanism was studied using most common isotherms models: Langmuir and Freundlich. The empirical Freundlich isotherm model describes adsorption on heterogeneous surfaces while Langmuir isotherm refers to homogeneous adsorption where all sites possess equal affinity for

Table 1
Models for kinetic and isotherm studies

Models	Equations	Linear forms	
Kinetic models			
Pseudo-first-order	$\frac{dq_e}{dt} = k_1\left(q_e - q_t\right)$	$\ln\left(q_e - q_t\right) - \ln q_e - k_1 t$	(3)
Pseudo-second-order	$\frac{dq_e}{dt} = k_2\left(q_e - q_t\right)^2$	$\frac{t}{q_t} = \frac{1}{k_2 q_e^2} + \frac{t}{q_e}$	(4)
Isotherm models			
Langmuir	$q_e = \frac{q_m K_L C_e}{1 + K_L C_e}$	$\frac{C_e}{q_e} = \frac{1}{K_L q_m} + \frac{C_e}{q_m}$	(5)
Freundlich	$q_e = K_F C_e^{1/n}$	$\ln q_e = \ln K_F + \frac{1}{n}\ln C_e$	(6)

adsorbate. Original and linear forms of these two models are given in Table 1 in which q_e and q_t (mg g^{-1}) are sorption capacities at equilibrium and at time t, respectively, k_1 and k_2 are rates constants of pseudo-first-order and pseudo-second-order models, respectively, C_e (mg L^{-1}) is hexavalent chromium concentration at equilibrium, q_m (mg g^{-1}) is theoretical maximum adsorbed amount, K_L (L mg^{-1}) is Langmuir constant and K_F is Freundlich empirical constant [27].

3. Results and discussion

3.1. Characterization of synthesized crosslinked chitosan films

The FTIR spectra of CS, CS-TPA 0.1% and 0.2% are shown in Fig. 3a. The disappearance of the peak at 1,690 cm^{-1} was attributed to the free aldehyde function and a strong peak at 1,640 cm^{-1} relative to the azomethine group CN confirmed that cross-linking agent successfully reacted with CS and Schiff bases were formed. A broad band was noted at 3,284 cm^{-1} corresponding to the overlapped O–H and N–H groups. On other hand, the presence of three characteristic polysaccharide bands at 1,150, 1,060 and 1,022 cm^{-1} were observed.

Scanning electron microscopy (SEM) images of CS films shown in Fig. 3b indicated that CS-TPA 0.2% film exhibited many irregularities and a compact porous structure in contrast to that of CS-TPA 0.1% which displayed a smooth and flat morphology without any cracks. This can be explained by covalent bridges caused by CS-TPA junctions, which created this arrangement during cross-linking process according to previous work.

Thermograms from differential scanning calorimetry (DSC) analysis of films are shown in Fig. 3c. Thermograms showed three endothermic peaks at 79.7°C, 57.7°C and 57.2°C of CS, CS-TPA 0.1% and CS-TPA 0.2% respectively, related to residual water evaporation. This agreed with previous studies [28,29]. Exothermic peaks at 291.0°C, 289.6°C and 295.5°C correspond to thermal degradation of CS, CS-TPA 0.1% and CS-TPA 0.2% respectively. Several studies have confirmed that degradation precedes fusion [28,29]. The dehydration of the saccharide rings and main degradation of pure or crosslinked CS film determined by the enthalpies of decomposition were 87.56, 41.9 and 68.95 J g^{-1} of CS, CS-TPA 0.1% and CS-TPA 0.2% respectively. Concerning glass transition temperature (T_g) of chitosan and derivatives, many findings reported different T_g values of 140°C, 183°C to 203°C [28,29]. In our case it was observed at around 150°C (Fig. 3c). For crosslinked CS, an increase in T_g was probably related to the effects of cross-linking which reduces mobility of chains.

3.2. Swelling properties

As shown in Fig. 4a, the swelling ratios of the prepared films increased rapidly during the first 10 min. This observation can be explained by a sponge effect exerted on first contact with water and then decreasing until establishment of an equilibrium state. This was 1 h in the current case. The swelling ratios were evaluated at 400%, 300% and 200% for CS, CS-TPA 0.1% and CS-TPA 0.2% respectively. This decrease in swelling rate is explained by the effect of cross-linking and cross-linking rate which increase the number of nodes in the network chain leading to a slowdown in water penetration and consequently the swelling ability was reduced. The chitosan film after its cross-linking thus becomes less hydrophilic. These trends agree with those reported by several authors who confirmed that swelling of crosslinked films depends on cross-linking rate as well as on the nature of the cross-linking agent [30–32]. Fig. 4b describes the swelling behavior of the three films at various temperatures 25°C, 40°C and 60°C at pH = 7. It was observed that an increase in temperature led to an increase in swelling rate due presumably to dissociation of hydrogen bonds between amino groups in the CS chain. This allowed for a relaxation of polymer chain and as result more water molecules were able to come inside the network [30].

A decrease in degree of swelling with increase in pH was observed (Fig. 4c). This meant that high swelling capacity is

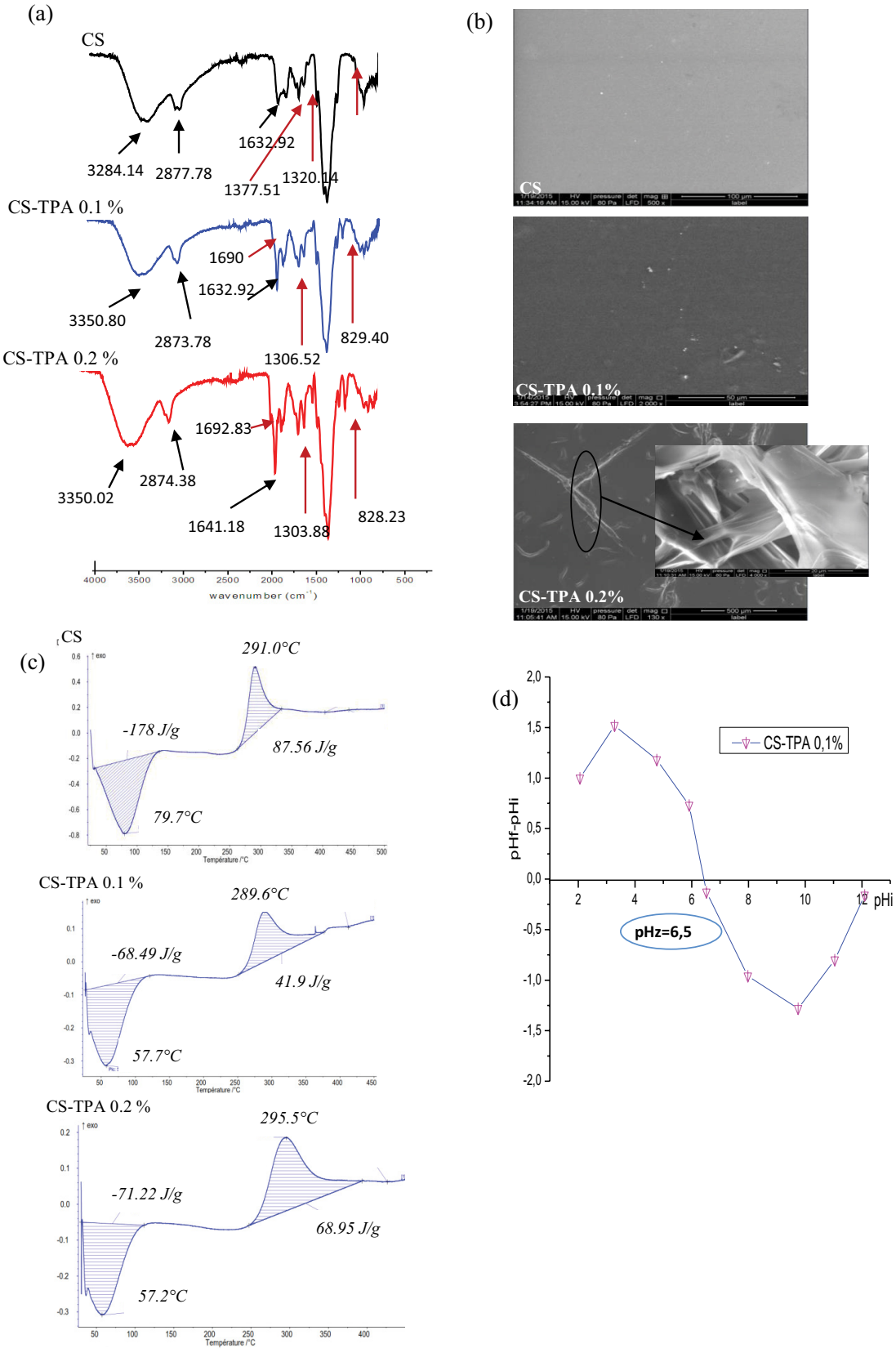

Fig. 3. Characterization of films: (a) FTIR spectra, (b) SEM photograms, (c) DSC thermograms and (d) determination of pH_{pzc} of CS-TPA 0.1% film.

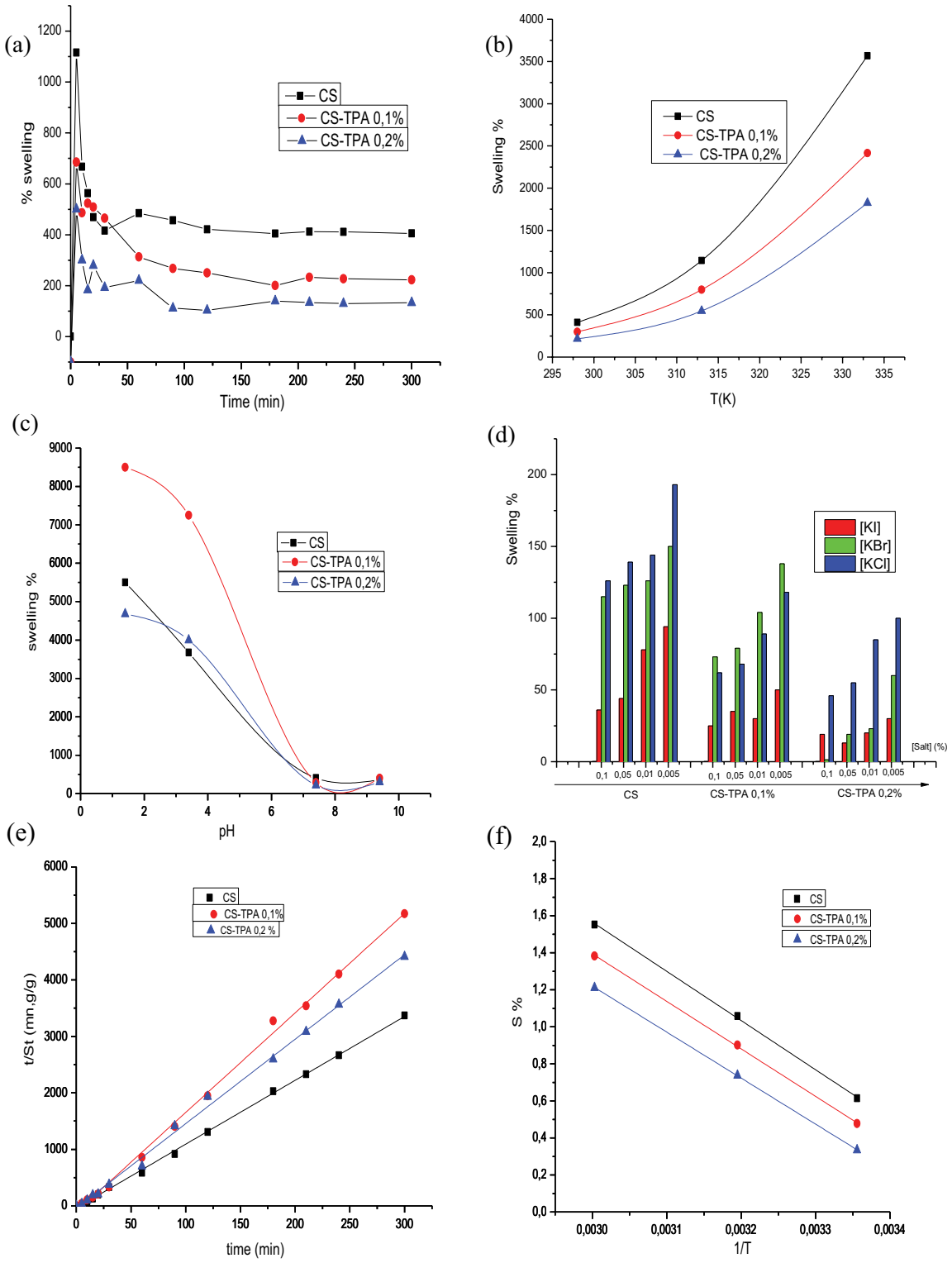

Fig. 4. Effect of (a) cross-linker rate, (b) temperature, (c) pH, (d) salinity on swelling behavior of the films: CS, CS-TPA 0.1%, CS-TPA 0.2%, (e) kinetic study of the swelling according to pseudo-second-order model and (f) thermodynamic study of the swelling.

obtained in acidic environments and is in line with results found by Li et al. [33] when investigating the swelling and mechanical properties of chitosan/GPTMS hydrogel films. CS is a weak polybase, therefore, in a low pH solution, CS amine functions are protonated which increases the electrostatic repulsions in the polymer network leading to the extension of the chain. This facilitates the penetration of more water molecules inside the network which results in a strong

swelling of the film. As pH increases, the degree of ionization of CS decreases and therefore, structure becomes more compact and lower swelling is observed.

The effect of salinity on swelling rate was investigated using KCl, KBr and KI salts at various concentrations (0.005, 0.01, 0.05, 0.1 M). As seen in Fig. 4d, a decrease in swelling ability was recorded with increasing concentrations of salt solutions. Indeed, at higher concentrations of NaCl solution, the osmotic pressure of the external solution increases, consequently the osmotic pressure difference between the external solution and the film decreases which makes it difficult for water molecules to penetrate the inner of the film. It was also noted that increasing radius of anion results in lower swelling. Therefore, the swelling behavior of the films CS and CS-TPA 0.2% in salt solutions can be classified in the following decreasing order KCl > KBr > KI. However, a change in swelling behavior of CS-TPA 0.1% was observed, the film showed highest values of swelling in KBr solutions. Similar results were obtained by Gierszewska and Ostrowska-Czubenko [33] when studying the swelling of chitosan membranes crosslinked by pentasodium tripolyphosphate (TPP) in various saline solutions at different concentrations. Additionally, the swelling decreased with crosslinker contents in salt solutions as in aqueous media. Similar trends have been reported in previous studied [33,34].

3.3. Kinetic and thermodynamic analysis of swelling

Kinetics were studied using pseudo-first-order and pseudo-second-order models, represented by Eqs. (7) and (8), respectively [30].

$$\ln\left(S_e - S_t\right) = \ln S_e - k_1 t \tag{7}$$

$$\frac{t}{S_t} = \frac{1}{k_2 S_e^2} + \frac{t}{S_e} \tag{8}$$

where S_e and S_t are quantity of water absorbed by films at equilibrium and at time t respectively. k_1 and k_2 are pseudo-first-order and pseudo-second-order absorption rate constants, respectively. The results obtained in Fig. 4e show a good coefficient of correlation with a pseudo-second kinetic order.

A thermodynamic study (Fig. 4f) made it possible to determine experimentally the parameters: Gibbs free energy ΔG, enthalpy ΔH and entropy ΔS using Van't Hoff expression, with the help of Eqs. (9) and (10) given:

$$\ln k_0 = \frac{\Delta S}{R} - \frac{\Delta H}{RT} \tag{9}$$

$$\Delta G = \Delta H - T\Delta S \tag{10}$$

where absorption equilibrium constant k_0 was determined from the amount of solvent absorbed per unit mass of films satisfies Van't Hoff equation [37]. Values of thermodynamic parameters are summarized in Table 2. ΔH values were positive for the three films indicating an exothermic Henry's process, which proceeds by creating new sites or pores in polymer. Positive ΔS values confirmed randomness at the solvent-film interface and negative values of ΔG showed that the swelling process was spontaneous.

3.4. Adsorption potential of synthesized films

The effect of the crosslinker concentration on the ability of chitosan films to remove Cr(VI) is shown in Fig. 5a. Adsorption of Cr(VI) onto CS-TPA 0.1% was rapid at first and reached equilibrium after 60 min. The adsorption capacity was estimated at 53 mg g^{-1} for CS-TPA 0.1% which was significantly higher than that of CS-TPA 0.2% at 33 mg g^{-1}. This difference was probably due to the more porous structure of CS-TPA 0.1%. So, for the further tests the CS-TPA 0.1% film was selected. It was also noted that the equilibrium time was independent of Cr(VI) initial concentration. This result was verified by others [35–37].

Fig. 5b reveals that the amount of hexavalent chromium adsorbed at equilibrium increases with an increase in initial Cr(VI) concentration. This behavior was attributed to the fact that with increasing initial Cr(VI) concentration, the difference in Cr(VI) concentration between the external solution and the adsorbent film increased. This favored the mass transfer between the liquid and solid phases and migration

Table 2
Kinetic and thermodynamic parameters of swelling process of the prepared films

Films	Kinetic data pseudo-second-order			Thermodynamic parameters			
	$k_2 \cdot 10^3$ (g mg^{-1} min^{-1})	$S_e \cdot 10^{-2}$ (g g^{-1})	R^2	T	ΔH (kJ mol^{-1})	ΔS (J K^{-1} mol^{-1})	ΔG (kJ mol^{-1})
CS	0.6	4.03	0.9992	298	–22.098	79.31	–1.537
				313			–2.726
				333			–4.312
CS-TPA 0.1%	0.4	2.91	0.9996	298	–21.327	75.57	–1.193
				313			–2.326
				333			–3.838
CS-TPA 0.2%	1.18	2.13	0.9999	298	–20.66	72.121	–0.832
				313			–1.914
				333			–3.356

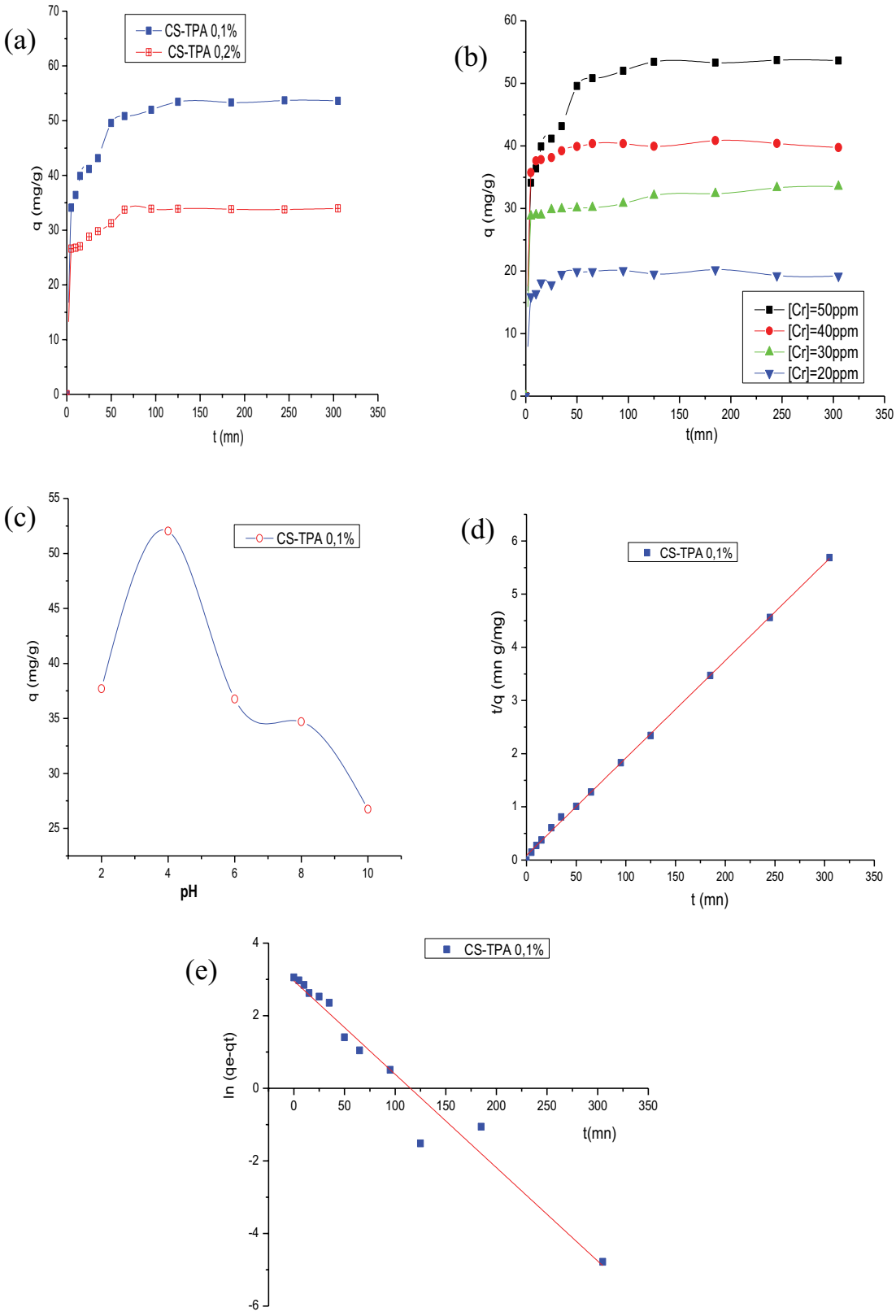

Fig. 5. Effect of (a) cross-linking rate, (b) initial Cr(VI) concentration, (c) pH on Cr(VI) removal by CS-TPA 0.1% film, kinetics modeling (d) pseudo-second-order and (e) pseudo-first-order.

of Cr(VI) ions to the surface of film and as a result the adsorption process improved [35].

The equations of pseudo-first-order as well as second were applied to determine the kinetic order of adsorption (Fig. 5c and d). The corresponding kinetic parameters are regrouped in Table 3.

Based on the correlation coefficient (R^2) values (0.9994, 0.9568 for pseudo-second-order, pseudo-first-order respectively), it was clear that adsorption of Cr(VI) on the crosslinked chitosan film was best fitted the pseudo-second-order model. In addition, the q_e value of the pseudo-second-order model was 54.615 mg g^{-1}, clearly closer to the experimental value. These findings suggested that the limiting step of Cr(VI) adsorption onto the synthesized film involves chemisorptions with the establishment of a strong electronic bond between chromium ions and the functional surface sites [38].

The increase in adsorption capacity at low pH could be explained by protonation of free amine groups in the films increasing electrostatic attractions with negatively charged aqueous forms ions $HCrO_4^-$, $Cr_2O_7^{2-}$, CrO_4^{2-}. The surface charge of adsorbent, pH_{pzc} of CS-TPA 0.1% film was approximately 6.5 (Fig. 3d). Below this value, the film surface was positively charged, and anionic adsorption of Cr(VI) occurred easily. Towards a neutral pH (i.e., 6→7), adsorption is a more complex process, and another mechanism could be involved, such as hydrophobic interactions, hydrogen bonds (film/Cr(VI)) and hydroxyl groups. This has also been observed at alkaline pH because the amino groups of the polymer are non-protonated. The optimal value for the adsorption of Cr(VI) by CS-TPA 0.1% films was found to be pH 4. As pH increased, adsorption capacity decreased due to the excess of OH^- ions competing with negative charge of anionic aqueous forms $HCrO_4^-$, $Cr_2O_7^{2-}$, CrO_4^{2-} to access the adsorption sites. At a pH above pH_{pzc}, the film surface has a negative charge leading to electrostatic repulsions between negative aqueous species and negatively charged film, resulting in a decrease in absorption of hexavalent chromium [40].

The absorption capacity of crosslinked films tested at 20°C, 30°C, 40°C and 50°C decreased with increasing solution temperature (Fig. 6a). This implied an exothermic process. It can be argued that the behavior could be attributed to shrinkage or/and alteration of active sites on the surface of the film at high temperature. As a result, the active adsorbent surface is reduced, and the adsorption efficiency declines. Also, the greater mobility of ions at high temperature strongly affects the probability of collision between metal ions and adsorbent sites and is in accordance with conclusions from previous studies [41].

The graph of $\ln k_0$ as a function of $1/T$, showed in Fig. 6b, allowed to calculate the enthalpy change and the entropy change. The calculated thermodynamic data are summarized in Table 3 and indicated the spontaneity of the Cr(VI) adsorption process on crosslinked chitosan films 0.1% (ΔG negative). The absolute value of $\Delta G°$ increased with temperature confirming that the spontaneous nature of the adsorption process increased with rising temperature. The negative values of ΔH demonstrated that the adsorption of chromium hexavalent on CS-TPA 0.1% films obtained by covalent cross-linking is of an exothermic nature and that the positive values of ΔS reveal an increase in randomness at the solid-solution interface.

The equilibrium data adjusted with Langmuir isotherm model are shown in Fig. 6c by plotting C_e/q_e as a function of C_e. The values q_{max} and K_L can be obtained from intersections and slopes. As it appears in Table 4, for crosslinked film CS-TPA 0.1%, the ratio C_e/q_e against C_e shows an approximate

Table 3
Kinetic and thermodynamic parameters for Cr(VI) adsorption on CS-TPA 0.1% film

			Kinetic parameters					Thermodynamic parameters		
			Pseudo-second-order		Pseudo-first-order					
			R^2 = 0.9994		R^2 = 0.9568			R^2 = 0.988		
	Cr(VI)		$k_2 \cdot 10^3$	q_e	$k_1 \cdot 10^2$	q_e		ΔH	ΔS	ΔG
Film	(ppm)	pH	(g mg^{-1} min^{-1})	(mg g^{-1})	(mn^{-1})	(mg g^{-1})	T (K)	(kJ mol^{-1})	(J K^{-1} mol^{-1})	(kJ mol^{-1})
CS-TPA 0.1%	50	4	3.786	54.615	2.573	19.29	293	–2.091	7.161	–4.189
							303			–4.26
							318			–4.368
							328			–4.439

Table 4
Isotherm parameters for Cr(VI) adsorption on CS-TPA 0.1% film

Film	Freundlich isotherm			Langmuir isotherm			
	n	K_F ($mg^{1-1/n}$ $L^{1/n}$ g^{-1})	R^2	q_{max} (mg g^{-1})	K_L (L mg^{-1})	R^2	R_L
CS-TPA 0.1%	4.00	16.50	0.974	60.53	0.094	0.996	0.175

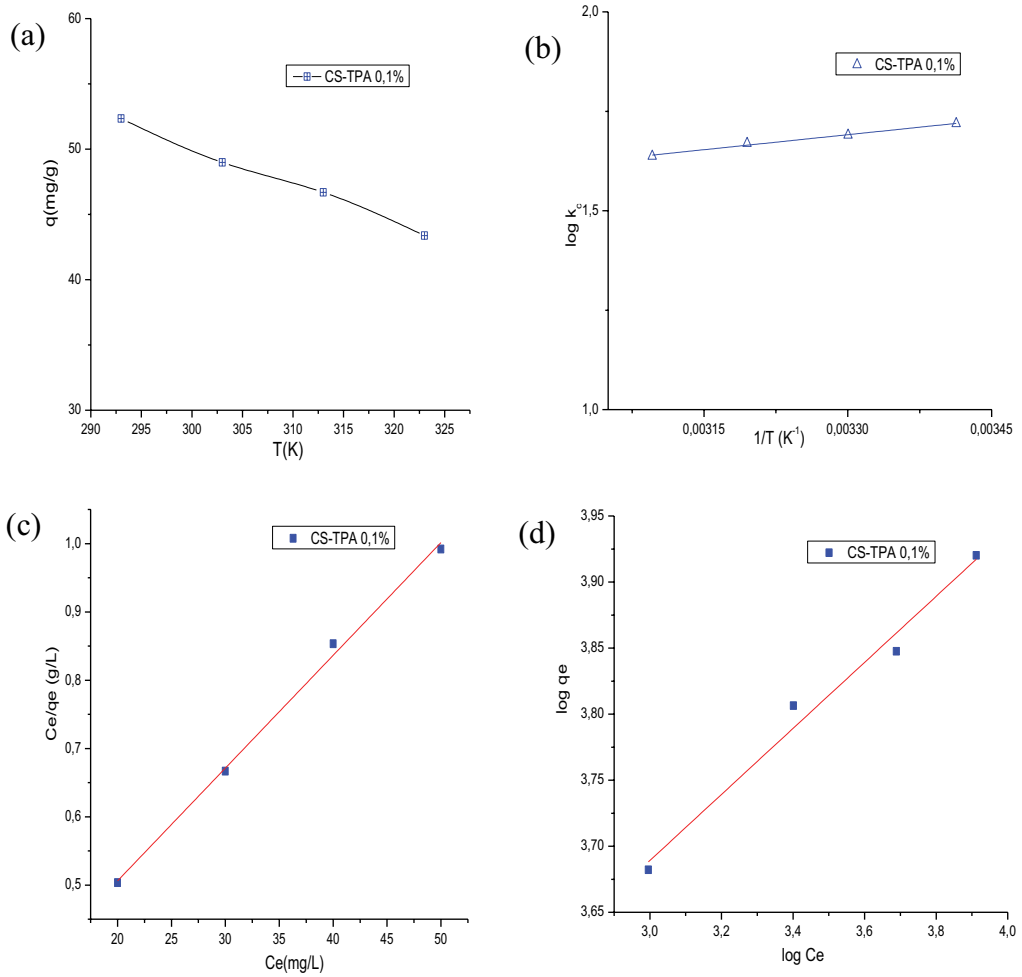

Fig. 6. (a) Effect of temperature on Cr(VI) removal by CS-TPA 0.1% film, (b) plot of logK_{eq} vs. 1/T, isotherms modeling, (c) Langmuir isotherm and (d) Freundlich isotherm.

Table 5
Comparison of adsorption capacities between CS-TPA 0.1% and other CS-based materials

CS biomaterials	q (mg g^{-1})	References
CS-Sodium dodecyl sulfate	09.5	[5]
CS-Activated carbon	24.4	[35]
CS-Nanoparticles Fe_2O_3	47.576	[36]
CS-Graphite binary composite	105.6	[37]
CS-Glutaraldehyde-coated bentonite	106.44	[38]
CS-Bentonite	89.13	[39]
CS-N,N′-Methylenebisacrylamide	149	[43]
CS-Terephthalaldehyde crosslinked	60.53	This study

linear relationship with a coefficient of determination (R^2 = 0.996). For the Freundlich model (Fig. 6d), factors K_F and 1/n were calculated from a curve of lnq_e against lnC_e, which gives an acceptable linear relationship with the R^2 of 0.974.

Thus, according to the isotherm analysis, adsorption of Cr(VI) on CS-TPA 0.1% films could be effectively simulated with the Langmuir isotherm model. The highest Langmuir's parameter value R_L was estimated at 0.175 which is less than 1 indicating a favorable adsorption [42].

The Langmuir's maximum adsorption capacity of Cr(VI) by CS-TPA 0.1% films was assessed to 60.53 mg g^{-1}. It can therefore be deduced that the adsorption of Cr(VI) on CS-TPA 0.1% films is a mono-layer physical adsorption which takes place onto a homogeneous surface. Table 5 summarizes the adsorption capacities (Langmuir's q_m) of modified chitosan materials against hexavalent chromium.

4. Conclusions

The present work has demonstrated that it is possible to synthesize adsorption films based on chitosan and crosslinked chitosan for removal of heavy metal pollutants. FTIR, SEM and DSC techniques confirmed the appearance of imine functions and the disappearance of aldehyde groups in crosslinked chitosan. The films exhibited sensitivity to variations in pH, temperature, and salinity. Investigation of the swelling behavior of materials revealed that swelling capacity of crosslinked chitosan was considerably less than that of non crosslinked

chitosan CS (400%, 300% and 200% for CS, CS-TPA 0.1% and CS-TPA 0.2%, respectively). The swelling behavior was pseudo-second-order. The performance of the synthesized films for hexavalent chromium removal was demonstrated. The results emphasized the effect of crosslinking on the efficiency of chitosan to remove Cr(VI) and the adsorption process was found to follow a pseudo-second-order kinetic model with a high correlation coefficient. Thermodynamic analysis revealed that adsorption of Cr(VI) onto CS-TPA 0.1% was spontaneous, exothermic with high randomness at solid/liquid interface during adsorption. The Langmuir's adsorption capacity of Cr(VI) by CS-TPA 0.1% film was found to be 60.53 mg g^{-1}.

In closing, the great potential of the synthesized crosslinked chitosan-based films for removal of hexavalent chromium was shown. Further investigations are required for evaluating the performance of the films under dynamic conditions.

References

[1] L. Pietrelli, I. Francolini, A. Piozzi, M. Sighicelli, I. Silvestro, M. Vocciante, Chromium(III) removal from wastewater by chitosan flakes, Appl. Sci., 10 (2020) 1925, doi: 10.3390/app10061925.

[2] W. Liu, H. Chen, A.G.L. Borthwick, Y. Han, J. Ni, Mutual promotion mechanism for adsorption of coexisting Cr(III) and Cr(VI) onto titanate nanotubes, Chem. Eng. J., 232 (2013) 228–236.

[3] S.L. Han, Y.A. Zang, Y. Gao, Q.Y. Yue, P. Zhang, W.J. Kong, B. Jin, X. Xu, B.Y. Gao, Co-monomer polymer anion exchange resin for removing Cr(VI) contaminants: adsorption kinetics, mechanism and performance, Sci. Total Environ., 709 (2020) 1–10, doi: 10.1016/j.scitotenv.2019.136002.

[4] F. Fu, Q. Wang, Removal of heavy metal ions from wastewaters: a review, J. Environ. Manage., 92 (2011) 407–418.

[5] X. Du, C. Kishima, H. Zhang, N. Miyamoto, N. Kano, Removal of chromium(VI) by chitosan beads modified with sodium dodecyl sulfate (SDS), Appl. Sci., 10 (2020) 4745, doi: 10.3390/app10144745.

[6] K. Yamada, Y. Ishiguro, Y. Kimura, H. Asamoto, H. Minamisawa, Two-step grafting of 2-hydroxyethyl methacrylate (HEMA) and 2-(dimethylamino)ethyl methacrylate (DMAEMA) onto a polyethylene plate for enhancement of Cr(VI) ion adsorption, Environ. Technol., 40 (2019) 855–869.

[7] Z. Cui, Y. Xiang, J. Si, M. Yang, Z. Qi, Z. Tao, Ionic interactions between sulfuric acid and chitosan membranes, Carbohydr. Polym., 73 (2008) 111–116.

[8] N. Boudouaia, Z. Bengharez, S. Jellali, Preparation and characterization of chitosan extracted from shrimp shells waste and chitosan film: application for Eriochrome black T removal from aqueous solutions, Appl. Water Sci., 9 (2019) 1–12, doi: 10.1007/s13201-019-0967-z.

[9] E. Khor, L.Y. Lim, Implantable applications of chitin and chitosan, Biomaterials, 24 (2003) 2339–2349.

[10] L. Illum, Chitosan and its use as a pharmaceutical excipient, Pharm. Res., 15 (2003) 1326–1331.

[11] M.N.V. Ravi Kumar, A review of chitin and chitosan applications, React. Funct. Polym., 46 (2000) 1–27.

[12] S.A. Agnihotri, N.N. Mallikarjuna, T.M. Aminabhavi, Recent advances on chitosan-based micro- and nanoparticles in drug delivery, J. Controlled Release, 100 (2004) 5–28.

[13] V.R. Sinha, A.K. Singla, S. Wadhawan, R. Kaushik, R. Kumria, K. Bansal, S. Dhawan, Chitosan microspheres as a potential carrier for drugs, Int. J. Pharm., 274 (2004) 1–33.

[14] S.-H. Lim, S.M. Hudson, Synthesis and antimicrobial activity of a water-soluble chitosan derivative with a fiber-reactive group, Carbohydr. Res., 339 (2004) 313–319.

[15] A.S. Shete, A.V. Yadav, S.M. Murthy, Chitosan and chitosan chlorhydrate based various approaches for enhancement of dissolution rate of carvedilol, DARU J. Pharm. Sci., 20 (2012) 93, doi: 10.1186/2008-2231-20-93.

[16] M.A. Basturk, Heat applied chitosan treatment on hardwood chips to improve physical and mechanical properties of particle board, Bio Resources, 7 (2012) 4858–4866.

[17] Q. Peng, M. Liu, J. Zheng, C. Zhou, Adsorption of dyes in aqueous solutions by chitosan–halloysite nanotubes composite hydrogel beads, Microporous Mesoporous Mater., 201 (2015) 190–201.

[18] K.F.B. Hossain, M.T. Sikder, M.M. Ahman, M.K. Uddin, M. Kurasaki, Investigation of chromium removal efficacy from tannery effluent by synthesized chitosan from crab shell, Arabian J. Sci. Eng., 42 (2017) 1569–1577.

[19] M. Rinaudo, Chitin and chitosan: properties and applications, Progr. Polym. Sci., 31 (2006) 603–632.

[20] H. Wu, X. Li, M. Nie, B. Li, Z. Jiang, Integral PVA-PES composite membranes by surface segregation method for pervaporation dehydration of ethanol, Chin. J. Chem. Eng., 19 (2011) 855–862.

[21] T. Uragami, T. Doi, T. Miyata, Chapter 18 – Pervaporation Properties of Surface-Modified Poly[(1-trimethylsilyl-1-propyne] Membranes, I. Pinnau, B.D. Freeman, Eds., Membrane Formation and Modification, American Chemical Society, 1999, pp. 263–279.

[22] M. Kumar Purkait, R. Singh, P. Mondal, D. Haldar, Chapter 13 – Applications of Thermal Induced Membrane Separation Processes, In: Thermal Induced Membrane Separation Processes, Elsevier, 2020, pp. 251–267.

[23] M.M. Beppu, R.S. Vieira, C.G. Aimoli, C.C. Santana, Crosslinking of chitosan membranes using glutaraldehyde: effect on ion permeability and water absorption, J. Membr. Sci., 301 (2007) 126–130.

[24] C. Wang, L. Yang, Y. He, H. Xiao, W. Lin, Microsphere-structured hydrogel crosslinked by polymerizable protein-based nanospheres, Polymer, 211 (2020) 123114, doi: 10.1016/j.polymer.2020.123114.

[25] E.-H. Jang, S.P. Pack, I. Kim, S. Chung, A systematic study of hexavalent chromium adsorption and removal from aqueous environments using chemically functionalized amorphous and mesoporous silica nanoparticles, Sci. Rep., 10 (2020) 5558, doi: 10.1038/s41598-020-61505-1.

[26] E. Díez-Peña, I. Quijada-Garrido, J.M. Barrales-Rienda, Analysis of the swelling dynamics of crosslinked P(*N*-iPAAm-*co*-MAA) copolymers and their homopolymers under acidic medium. a kinetics interpretation of the overshooting effect, Macromolecules, 36 (2003) 2475–2483.

[27] X. Guo, A. Liu, J. Lu, X. Niu, M. Jiang, Y. Ma, X. Liu, M. Li, Adsorption mechanism of hexavalent chromium on biochar: kinetic, thermodynamic, and characterization studies, ACS Omega, 5 (2020) 27323–27331.

[28] K. Sakurai, T. Maegawa, T. Takahashi, Glass transition temperature of chitosan and miscibility of chitosan/poly(*N*-vinyl pyrrolidone) blends, Polymer, 41 (2000) 7051–7056.

[29] Y. Dong, Y. Ruan, H. Wang, Y. Zhao, D. Bi, Studies on glass transition temperature of chitosan with four techniques, J. Appl. Polym. Sci., 93 (2004) 1553–1558.

[30] J. Ostrowska-Czubenko, M. Gierszewska, M. Pieróg, pH-responsive hydrogel membranes based on modified chitosan: water transport and kinetics of swelling, J. Polym. Res., 22 (2015) 153, doi: 10.1007/s10965-015-0786-3.

[31] J. Berger, M. Reist, J.M. Mayer, O. Felt, N.A. Peppas, R. Gurny, Structure and interactions in covalently and ionically crosslinked chitosan hydrogels for biomedical applications, Eur. J. Pharm. Biopharm., 57 (2004) 19–34.

[32] M. Gierszewska-Drużyńska, J. Ostrowska-Czubenko, Structural and swelling properties of hydrogel membranes based on chitosan crosslinked with glutaraldehyde and sodium tripolyphosphate, Progr. Chem. Appl. Chitin Derivatives, XX (2015) 43–53.

[33] M. Gierszewska, J. Ostrowska-Czubenko, Equilibrium swelling study of crosslinked chitosan membranes in water, buffer and

salt solutions, Progr. Chem. Appl. Chitin Derivatives, XXI (2016) 55, doi: 10.15259/PCACD.21.05.
[34] A. Bibi, S.-ur Rehman, R. Faiz, T. Akhtar, M. Nawaz, S. Bibi, Effect of surfactants on swelling capacity and kinetics of alginate-chitosan/CNTs hydrogel, Mater. Res. Express, 6 (2019) 085065.
[35] E. Serpil, Comparison of chitosan-based biocomposites for remediation of water with Cr(VI) ions, Iran. J. Chem. Chem. Eng., 39 (2020) 245–251.
[36] T. Altun, H. Ecevit, Cr(VI) removal using Fe_2O_3-chitosan-cherry kernel shell pyrolytic charcoal composite beads, Environ. Eng. Res., 25 (2020) 426–438.
[37] R. Dongre, Adsorption of hexavalent chromium by graphite–chitosan binary composite, Bull. Mater. Sci., 39 (2016) 865–874.
[38] T. Altun, Preparation and application of glutaraldehyde crosslinked chitosan coated bentonite clay capsules: chromium(VI) removal from aqueous solution, J. Chil. Chem. Soc., 65 (2020) 4790–4797.
[39] H. Moussout, H. Ahlafi, M. Aazza, C. El Akili, Performances of local chitosan and its nanocomposite 5%bentonite/chitosan in the removal of chromium ions (Cr(VI)) from wastewater, Int. J. Biol. Macromol., 108 (2018) 1063–1073.
[40] T. Altun, H. Ecevit, Y. Kar, Ç. Birsen, Adsorption of Cr(VI) onto crosslinked chitosan-almond shell biochars: equilibrium, kinetic, and thermodynamic studies, J. Anal. Sci. Technol., 12 (2021), doi: 10.1186/s40543-021-00288-0.
[41] N. Nordine, Z. El Bahri, H. Sehil, R.I. Fertout, Z. Rais, Z. Bengharez, Lead removal kinetics from synthetic effluents using Algerian pine, beech and fir sawdust's: optimization and adsorption mechanism, Appl. Water Sci., 6 (2016) 349–358.
[42] K.Y. Foo, B.H. Hameed, Insights into the modeling of adsorption isotherm systems, Chem. Eng. J., 156 (2010) 2–10.
[43] M.N.M. Ismael, A. El Nemr, E.S.H. El Ashry, H. Abdel Hamid, Removal of hexavalent chromium by cross-linking chitosan and *N,N'*-methylene bis-acrylamide, Environ. Process., 7 (2020) 911–930.